# *LBD18/ASL20* Regulates Lateral Root Formation in Combination with *LBD16/ASL18* Downstream of *ARF7* and *ARF19* in Arabidopsis[1][C][W][OA]

**Han Woo Lee, Nan Young Kim, Dong Ju Lee, and Jungmook Kim***

Department of Plant Biotechnology and Agricultural Plant Stress Research Center, Chonnam National University, Buk-Gu, Gwangju 500–757, Korea

The *LATERAL ORGAN BOUNDARIES DOMAIN/ASYMMETRIC LEAVES2-LIKE* (*LBD/ASL*) genes encode proteins harboring a conserved amino acid domain, referred to as the LOB (for lateral organ boundaries) domain. While recent studies have revealed developmental functions of some *LBD* genes in Arabidopsis (*Arabidopsis thaliana*) and in crop plants, the biological functions of many other *LBD* genes remain to be determined. In this study, we have demonstrated that the *lbd18* mutant evidenced a reduced number of lateral roots and that *lbd16 lbd18* double mutants exhibited a dramatic reduction in the number of lateral roots compared with *lbd16* or *lbd18*. Consistent with this observation, significant β-glucuronidase (GUS) expression in $Pro_{LBD18}$*:GUS* seedlings was detected in lateral root primordia as well as in the emerged lateral roots. Whereas the numbers of primordia of *lbd16*, *lbd18*, and *lbd16 lbd18* mutants were similar to those observed in the wild type, the numbers of emerged lateral roots of *lbd16* and *lbd18* single mutants were reduced significantly. *lbd16 lbd18* double mutants exhibited additively reduced numbers of emerged lateral roots compared with single mutants. This finding indicates that *LBD16* and *LBD18* may function in the initiation and emergence of lateral root formation via a different pathway. LBD18 was shown to be localized into the nucleus. We determined whether LBD18 functions in the nucleus using a steroid regulator-inducible system in which the nuclear translocation of LBD18 can be regulated by dexamethasone in the wild-type, *lbd18*, and *lbd16 lbd18* backgrounds. Whereas *LBD18* overexpression in the wild-type background induced lateral root formation to some degree, other lines manifested the growth-inhibition phenotype. However, *LBD18* overexpression rescued lateral root formation in *lbd18* and *lbd16 lbd18* mutants without inducing any other phenotypes. Furthermore, we demonstrated that *LBD18* overexpression can stimulate lateral root formation in *auxin response factor7/19* (*arf7 arf19*) mutants with blocked lateral root formation. Taken together, our results suggest that *LBD18* functions in the initiation and emergence of lateral roots, in conjunction with *LBD16*, downstream of *ARF7* and *ARF19*.

The *LATERAL ORGAN BOUNDARIES DOMAIN/ASYMMETRIC LEAVES2-LIKE* (*LBD/ASL*) genes (hereafter referred to as *LBD*) encode proteins harboring a LOB (for lateral organ boundaries) domain, which is a conserved amino acid domain that is detected only in plants, indicative of its function in plant-specific processes (Iwakawa et al., 2002; Shuai et al., 2002). There are 42 Arabidopsis (*Arabidopsis thaliana*) *LBD* genes, which have been assigned to two classes. Class I comprises 36 genes and class II comprises six genes (Iwakawa et al., 2002; Shuai et al., 2002). The class I proteins harbor LOB domains similar to those observed in the LOB protein, whereas the class II proteins are less similar to the class I proteins, which include the LOB domain as well as regions outside of the LOB domain. The LOB domain is approximately 100 amino acids in length and harbors a conserved 4-Cys motif with $CX_2CX_6CX_3C$ spacing, a Gly-Ala-Ser block, and a predicted coiled-coil motif with $LX_6LX_3LX_6L$ spacing, reminiscent of the Leu zipper found in the majority of class I proteins (Shuai et al., 2002). None of the class II proteins were predicted to form coiled-coil structures.

Although we currently understand very little about the biological roles of the *LBD* genes, there have been some reports describing the developmental functions of *LBD* genes in Arabidopsis on the basis of gain-of-function studies. The gain-of-function mutants of *LBD36/ASL1*, designated *downwards siliques1*, showed shorter internodes and downward lateral organs such as flowers (Chalfun-Junior et al., 2005). Although the *lbd36* loss-of-function mutants did not show morphological phenotypes, the analysis of *lbd36 as2* double

[1] This work was supported by the Plant Diversity Research Center of the 21st Century Frontier Research Program (grant no. PF06302–01), by the Agricultural Plant Stress Research Center (grant no. R11–2001–092–04001–0), and by the World Class University project funded by the Ministry of Education, Science and Technology (grant no. R31–2009–000–20025–0) to J.K.

* Corresponding author; e-mail jungmkim@chonnam.ac.kr.

The author responsible for distribution of materials integral to the findings presented in this article in accordance with the policy described in the Instructions for Authors (www.plantphysiol.org) is: Jungmook Kim (jungmkim@chonnam.ac.kr).

[C] Some figures in this article are displayed in color online but in black and white in the print edition.

[W] The online version of this article contains Web-only data.

[OA] Open Access articles can be viewed online without a subscription.

www.plantphysiol.org/cgi/doi/10.1104/pp.109.143685

mutants showed that these two members act redundantly to control cell fate determination in the petals. Another Arabidopsis gain-of-function mutant, *jagged lateral organs-D* (*jlo-D*), generates strongly lobed leaves and the shoot apical meristem prematurely arrests organ initiation, terminating in a pin-like structure (Borghi et al., 2007). During embryogenesis, *JLO* (=*LBD30/ASL19*) is necessary for the initiation of cotyledons and development beyond the globular stage. The results of misexpression experiments indicate that during postembryonic development, *JLO* function is required for the initiation of plant lateral organs. A recent study showed that the LOB domain of AS2 cannot be functionally replaced by those of other members of the LOB family, indicating that dissimilar amino acid residues in the LOB domains are important for characteristic functions of the family members (Matsumura et al., 2009).

Thirty-five *LBD* genes in rice (*Oryza sativa*) have been identified from the genome sequences of the two rice subspecies, a *japonica* rice (Nippobare) and an *indica* rice (9311; Yang et al., 2006). Analyses of rice mutants have provided evidence of the involvement of a variety of rice *LBD* genes in lateral organ development. *CROWN ROOTLESS1* (*CRL1*), encoding a LBD protein, is crucial for crown root formation in rice (Inukai et al., 2005). The *crl1* mutant showed auxin-related phenotypes, such as decreased lateral root number, auxin insensitivity in lateral root formation, and impaired root gravitropism. A rice AUXIN RESPONSE FACTOR (ARF) appears to directly regulate *CRL1* expression in the auxin signaling pathway (Inukai et al., 2005). *ADVENTITIOUS ROOTLESS1* encodes an auxin-responsive protein with a LOB domain that controls the initiation of adventitious root primordia in rice and turned out to be the same gene as *CRL1* (Liu et al., 2005).

Lateral roots of Arabidopsis are derived from a subset of the pericycle cells (pericycle founder cells), which are positioned at the xylem poles within the parent root tissues (Casimiro et al., 2003). The mature pericycle cells dedifferentiate to form lateral root primordium (LRP), which undergoes consistent anticlinal and periclinal cell divisions to generate a highly organized LRP (Malamy and Benfey, 1997). The LRP emerges from the parent root via cell expansion, and the activation of the lateral root meristem results in continued growth of the organized lateral root. A growing body of physiological and genetic evidence has been collected to suggest that auxin plays a profound role in lateral root formation. For example, many auxin-related mutants have been shown to affect lateral root formation (Casimiro et al., 2003). Lateral root formation in Arabidopsis was shown to be regulated by ARF7 and ARF19 via the direct activation of *LBD16* and *LBD29/ASL16* (Okushima et al., 2007). Overexpression of *LBD16* and *LBD29* induced lateral root formation in the absence of ARF7 and ARF19, and the dominant repression of *LBD16* inhibited lateral root formation, thus suggesting that these LBDs function downstream of ARF7- and ARF19-mediated auxin signaling during lateral root formation. The results of selection and binding assays demonstrated that a truncated LOB protein harboring only the conserved LOB domain can preferentially bind to unique DNA sequences, which is indicative of a DNA-binding protein (Husbands et al., 2007). Recently, *LBD18* was shown to regulate tracheary element differentiation (Soyano et al., 2008).

In this study, we demonstrated that *LBD18* is involved in the regulation of lateral root formation, based on the analysis of loss-of-function mutants and the complementation of *lbd18* and *lbd16 lbd18* mutants by dexamethasone (DEX)-inducible *LBD18* expression. Double mutations in *LBD16* and *LBD18* resulted in a synergistic reduction in the number of lateral roots, particularly in initiation and emergence, compared with either the *lbd16* or *lbd18* single mutant. This finding is suggestive of a combinatorial interaction of *LBD16* and *LBD18* in the process of lateral root formation. *LBD18* expression in *arf7* and *arf19* mutants by the DEX-inducible system increased the number of lateral roots, thus demonstrating that *LBD18* functions downstream of *ARF7* and *ARF19* in lateral root formation.

## RESULTS

### Phenotype Analysis of *lbd16*, *lbd18*, and *lbd16 lbd18* Mutants

In an earlier study, we constructed a transgenic Arabidopsis that expressed the glucocorticoid receptor (GR)-fused stabilized indoleacetic acid1 (iaa1) protein harboring an amino acid change in domain II (Park et al., 2002). DEX treatment of this transgenic Arabidopsis evoked dramatic auxin-related phenotypes and repressed the auxin induction of a variety of *Aux/IAA* genes (Park et al., 2002; Ku et al., 2009). We previously assessed the effects of DEX-inducible iaa1 on auxin-regulated gene expression, focusing on early genes, with the Affymetrix full genome array and subsequently identified a transcriptome downstream of iaa1 during the auxin response (Lee et al., 2009). In order to characterize the biological functions of auxin response genes downstream of iaa1, we analyzed a variety of Arabidopsis T-DNA insertion mutants, but none of them evidenced notable morphological phenotypes. Then, we constructed double mutants of similarly classified single mutants and examined auxin-related phenotypes (data not shown). We found that among them, *lbd16-1 lbd18-1* double mutants exhibited significantly reduced numbers of lateral roots. Figure 1, A and B, show the schematic view and the results of PCR analysis of the homozygous T-DNA insertion mutants of *lbd16-1* and *lbd18-1* single mutants. Figure 1C shows the results of reverse transcription (RT)-PCR analysis of homozygous T-DNA insertion mutants of *lbd16-1* and *lbd18-1* as well as *lbd16-1 lbd18-1*. We examined the

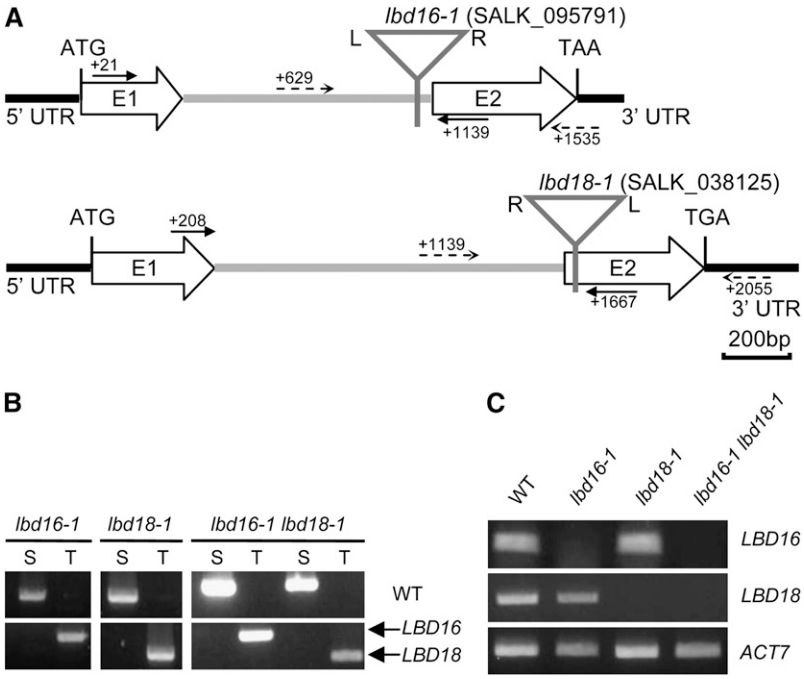


**Figure 1.** PCR analysis of the *lbd16*, *lbd18*, and *lbd16 lbd18* mutants. A, Location of T-DNA insertions of *LBD16* and *LBD18* in Arabidopsis. T-DNA insertions are indicated by triangles. *LBD16* and *LBD18* are composed of two exons indicated by E1 and E2 and one intron indicated by the gray lines. Solid lines and dotted lines indicate the locations of the primers for the RT-PCR and the primers for the PCR of genomic DNA, respectively. Numbers indicate the position of the first nucleotide of each primer relative to the AUG initiation codon. L and R, Left and right borders of T-DNA; UTR, untranslated region. B, PCR analysis of T-DNA insertion mutants. Genomic DNA isolated from each mutant was subjected to PCR with primers specific for *LBD16* or *LBD18* and the primers for T-DNA. S and T, PCR products amplified by specific primers (S) or specific primers and T-DNA primers (T); WT, wild-type Columbia. C, RT-PCR analysis of T-DNA insertion mutants. Total RNA isolated from 7-d-old light-grown seedlings was subjected to RT-PCR. The *ACTIN7* mRNA was utilized as a loading control.

auxin-related phenotypes and morphological changes of these single mutants but detected no significant phenotypes except for the change in lateral root formation. One example demonstrates the insignificant difference in root growth inhibition between these mutants and the wild-type plants, with varying concentrations of indole-3-acetic acid (IAA; Supplemental Fig. S1). However, we did note a significant reduction in lateral root number for *lbd18-1* as well as *lbd16-1* when compared with the wild-type plants at 5 and 8 d after germination (Fig. 2, A–C). The *lbd16-1 lbd18-1* double mutants showed substantially reduced numbers of lateral roots compared with *lbd16-1* and *lbd18-1* by dissecting microscopy. The addition of the auxin 2,4-dichlorophenoxyacetic acid (2,4-D) to the *lbd16-1*, *lbd18-1*, and *lbd16-1 lbd18-1* mutants rescued the reduced lateral root number to wild-type levels (Fig. 2D). These results indicate that *LBD18*, in combination with *LBD16*, is involved in lateral root formation during the auxin response.

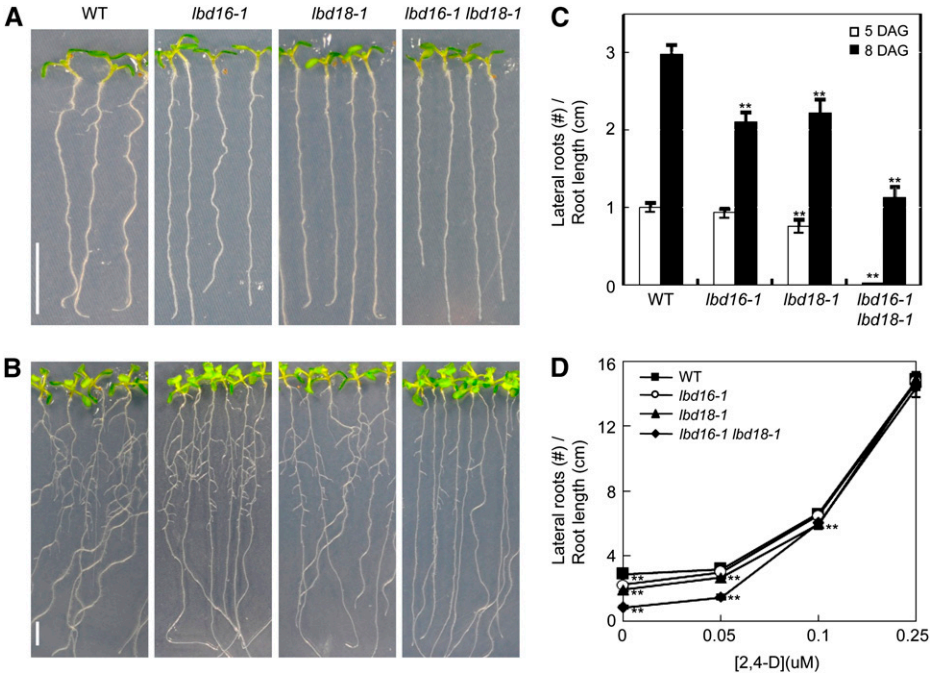


**Figure 2.** Lateral root phenotypes of *lbd16*, *lbd18*, and *lbd16 lbd18* mutants. A and B, Lateral roots of T-DNA insertion mutants and the wild type (WT). Photographs were taken 5 d (A) or 8 d (B) after germination. Bars = 1 cm. C, Number of lateral roots at different days after germination (DAG). The white columns and black columns indicate the lateral root numbers of plants grown vertically 5 and 8 d after germination, respectively. $n > 29$. Lateral roots were counted with a dissecting microscope. Lateral root numbers per unit root length (cm) measured were plotted. D, Number of lateral roots with varying concentrations of 2,4-D. Lateral root numbers of 5-d-old seedlings grown vertically were counted 4 d after transfer to medium containing the indicated concentrations of 2,4-D. $n > 18$. Lateral root numbers per unit root length (cm) measured were plotted. Asterisks denote statistical significance at $P < 0.01$.

### GUS Expression Patterns of $Pro_{LBD16}$:*GUS* and $Pro_{LBD18}$:*GUS* Transgenics

It has been previously reported that in $Pro_{LBD16}$:*GUS* seedlings, strong GUS activity was detected in the root stele and the lateral root primordia (Okushima et al., 2007). We additionally assessed the expression of GUS at three different stages of lateral primordium formation (Malamy and Benfey, 1997) and during lateral root emergence in transgenic Arabidopsis harboring the 1.4-kb *LBD16* promoter-*GUS* fusion construct ($Pro_{LBD16}$:*GUS*) that we generated (Fig. 3, A–D). We noted strong GUS expression not only in the root stele (Fig. 3, A–D) and the lateral root primordia (Fig. 3B) but also in the developing (Fig. 3B), emerged (Fig. 3C), and mature (Fig. 3D) lateral roots in 7-d-old light-grown $Pro_{LBD16}$:*GUS* seedlings. Upon treatment with the auxin IAA, strongly enhanced GUS expression was detected in the primary roots and lateral roots (Fig. 3, A and D, bottom panels). We noted intense GUS expression in developing primordia (Fig. 3B, bottom panels). In order to understand the role of *LBD18* in lateral root formation, we generated transgenic Arabidopsis harboring the 2.0-kb *LBD18* promoter-*GUS* fusion construct ($Pro_{LBD18}$:*GUS*) and examined GUS expression during lateral primordium formation and lateral root emergence (Fig. 3, E–H). In 7-d-old light-grown $Pro_{LBD18}$:*GUS* seedlings, significant GUS activity was noted in the root stele (Fig. 3E), similar to what was noted in the $Pro_{LBD16}$:*GUS* seedlings. The GUS

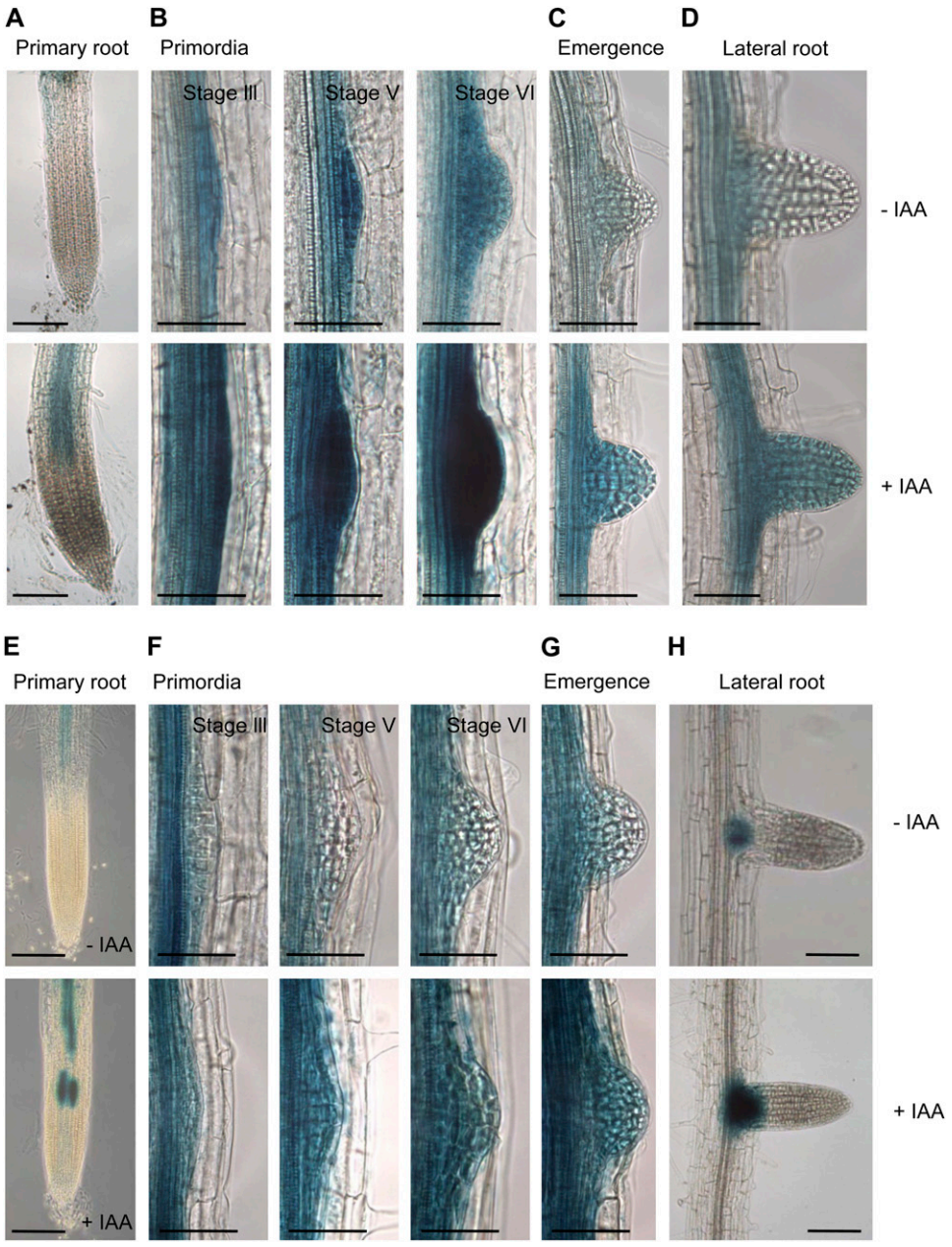


**Figure 3.** GUS expression in $Pro_{LBD16}$:*GUS* and $Pro_{LBD18}$:*GUS* transgenics. A to D, GUS expression in 7-d-old light-grown $Pro_{LBD16}$:*GUS* seedlings. Seedlings were incubated without or with 20 $\mu$M IAA for 4 h. Images were obtained after 8 h of incubation with 5-bromo-chloro-3-indolyl glucuronide. E to H, GUS expression in 7-d-old light-grown $Pro_{LBD18}$:*GUS* seedlings. Seedlings were incubated without or with 20 $\mu$M IAA for 8 h. Images were obtained after 16 h of incubation with 5-bromo-chloro-3-indolyl glucuronide. A and E, GUS expression of a primary root without or with IAA. Bars = 100 mm. B and F, GUS expression of primordia of the developing lateral root without or with IAA. C and G, GUS expression of an emerged lateral root without or with IAA. D and H, GUS expression of a lateral root without or with IAA. Stages of lateral roots were based on Malamy and Benfey (1997). Bars = 50 mm.

staining patterns of $Pro_{LBD18}$:*GUS* seedlings were also assessed for three different stages of lateral root development. GUS activity was observed in the lateral root primordia as well as the emerging lateral root (Fig. 3, F and G). However, no GUS activity was detected in the lateral root stele (Fig. 3H). Treatment with the auxin IAA resulted in enhanced GUS expression in the primary and lateral roots (Fig. 3, E–H, bottom panels). These GUS expression patterns are consistent with the role of *LBD18* in lateral root formation during the auxin response. Overlapping GUS expression patterns of $Pro_{LBD16}$:*GUS* and $Pro_{LBD18}$:*GUS* during the formation of lateral root primordium and during lateral root emergence suggest a common function in lateral root initiation and emergence.

### Analysis of Primordia and Emerged Lateral Roots in *lbd16*, *lbd18*, and *lbd16 lbd18* Mutants

Lateral root development can be divided into four steps: stimulation and dedifferentiation of pericycle cells, ordered cell division and redifferentiation to generate a highly organized lateral root primordium, emergence of the lateral root primordium via cell expansion, and activation of the lateral root meristem to permit the continued growth of the organized lateral root (Malamy and Benfey, 1997; Casimiro et al., 2003). In order to determine the step of lateral root formation in which *LBD16* and *LBD18* act, we enumerated the lateral root primordia and emerged lateral roots of *lbd16-1*, *lbd18-1*, and *lbd16-1 lbd18-1* mutants by photographing the roots with a light microscope equipped with a camera. As shown in Figure 4, the numbers of primordia in the *lbd16* and *lbd18* single or double mutants were similar to the numbers observed in the wild type. However, the numbers of emerged lateral roots of *lbd16* and *lbd18* single mutants were significantly reduced as compared with the wild type. The *lbd16 lbd18* double mutants exhibited additively reduced numbers of emerged lateral roots compared with the single mutants. We further analyzed the effects of *lbd16* and *lbd18* mutations on primordium development by counting the numbers of primordia from stage I to stage VIII on the basis of the classification made by Malamy and Benfey (1997), showing that primordium development was not significantly affected at every stage examined (Fig. 4B). These results suggest that *LBD16* and *LBD18* may be involved in the initiation and emergence of lateral roots.

### Gain-of-Function Analysis of *LBD16* and *LBD18*

GFP fusion proteins LBD16 and LBD18 are localized in the nucleus in protoplasts isolated from Arabidopsis mesophyll cells (Fig. 5). To evaluate the gain-of-function phenotypes of LBD16 and LBD18 in the nucleus, we utilized a steroid regulator-inducible system via fusion of the full-length coding region of LBD16 or LBD18 in-frame with the hormone-binding domain of the GR to generate transgenic Arabidopsis ($Pro_{35S}$:*LBD16*:*GR* or $Pro_{35S}$:*LBD18*:*GR*) in the ecotype Columbia (Col-0) wild-type background. As observed in the RNA gel-blot analysis of these transgenic lines, two bands corresponding to endogenous *LBD16* or *LBD18* and *LBD16*:*GR* or *LBD18*:*GR* transcripts were detected, and the transgenic lines exhibiting high expression ratios of the *GR* fusion transcripts over the endogenous *LBD16* or *LBD18* transcripts (indicated by black triangles) were selected for phenotype analysis (Fig. 6A). DEX treatment significantly stimulated lateral root numbers in all four lines of $Pro_{35S}$:*LBD16*:*GR* transgenic plants when compared with the

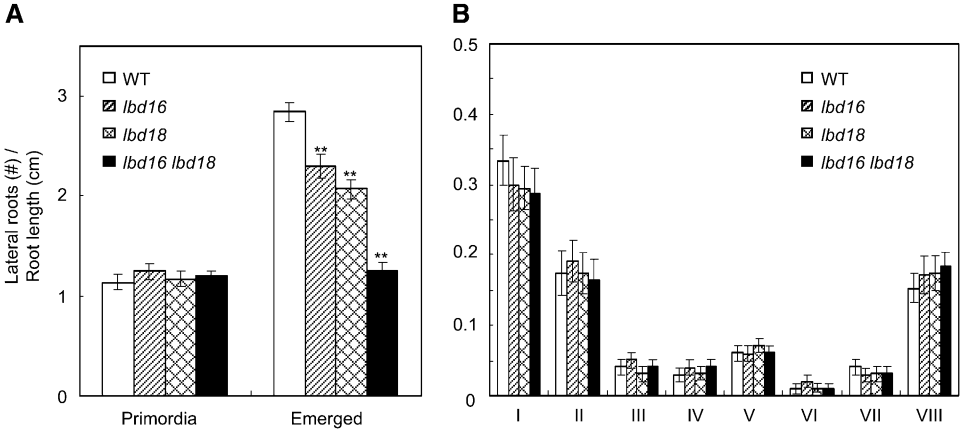


**Figure 4.** Numbers of lateral roots of *lbd16*, *lbd18*, and *lbd16 lbd18* mutants. A, Numbers of primordia of lateral roots or emerged lateral roots. Plants were grown vertically for 8 d after germination. Primordia or emerged lateral roots were photographed with a camera affixed to a Leica CME trinocular light microscope at 100- or 400-fold magnification and counted on the basis of Malamy and Benfey (1997). $n > 10$ per column. Asterisks denote statistical significance at $P < 0.01$. WT, Wild type. B, Numbers of primordia at given stages before emergence of lateral roots. Stages I to VIII of primordia were based on the classification by Malamy and Benfey (1997).

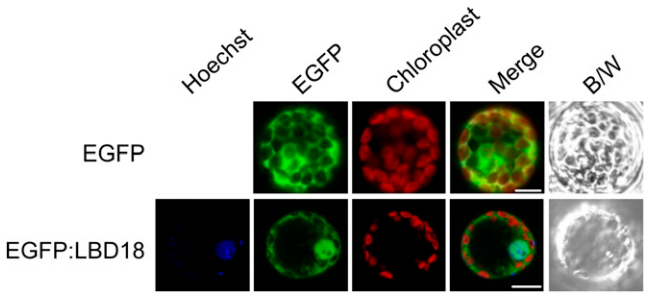


**Figure 5.** Nuclear localization of EGFP fusion proteins of LBD18. Images represent epifluorescence (EGFP), autofluorescence (chloroplast), merged, and black and white (B/W) field images of mesophyll protoplasts transfected with plasmid DNAs. Bars = 10 $\mu$m.

wild-type plants as well as in the absence of DEX (Fig. 6, B and C). This observation is similar to a previous report describing the stimulation of lateral root formation via *LBD16* overexpression in *arf7 arf19* mutants (Okushima et al., 2007). In contrast, two lines (lines 14-7 and 38-2) of *Pro*$_{35S}$*:LBD18:GR* transgenic plants in the presence of DEX exhibited severely reduced root length and lateral root numbers, and the 25-2 line showed some degree of reduction in both root length and lateral root number (Fig. 6, B and D; Supplemental Fig. S2). When the DEX concentrations were varied from 0.25 to 5 $\mu$M with the 38-2 and 25-2 lines, similar results showing dose-response curves were generated (Supplemental Fig. S3). The 13-3 line, which expresses the lowest levels of the *LBD18:GR* transcripts among the lines tested, showed insignificant changes in both root length and lateral root number upon treatment with DEX. These findings demonstrated that the expression levels of the *LBD18:GR* transcripts are correlated with phenotype severity in the roots. However, when we examined the 28-9 line, which expresses lower levels of the *LBD18:GR* transcripts than both the 14-7 and 38-2 lines but higher levels of the transcripts than the 13-3 line, we noted statistically significant stimulations of lateral root number by various concentrations of DEX (Fig. 6E). These results indicate that appropriate levels of *LBD18* expression may be required for the stimulation of lateral root formation, but higher levels of *LBD18* expression could result in the inhibition of primary and lateral roots. These results also showed that LBD18 as well as LBD16 function in the nucleus to regulate lateral root formation. In addition, consistent with the observed inhibition of root growth with high levels of *LBD18* expression, the hypocotyl lengths of four different lines of *Pro*$_{35S}$*:LBD18:GR* transgenic plants were reduced significantly by DEX treatment (Fig. 7).

### Overexpression of *LBD18* Rescues Lateral Root Formation of *lbd18* Single Mutants and *lbd16 lbd18* Double Mutants

Although we have observed statistically significant increases in the numbers of lateral roots in *Pro*$_{35S}$*:LBD18:GR* transgenic plants (the 28-9 line) with various concentrations of DEX (Fig. 6E), other lines evidenced severe root growth inhibition phenotypes. To address this mixed phenotype problem, we attempted to determine whether *LBD18* could rescue the wild-type phenotype in *lbd18* and *lbd16 lbd18* mutants using *Pro*$_{35S}$*:LBD18:GR*. Transgenic *lbd18* or *lbd16 lbd18* mutants expressing *LBD18:GR* transcripts were generated by crossing the mutants with *Pro*$_{35S}$*:LBD18:GR*, as demonstrated by the T-DNA insertions and expression patterns of *LBD18:GR* and *LBD18* (Fig. 8A). Quantitative RT-PCR analysis of the *LBD18* transcripts demonstrated that the transgenic mutant plants express the *LBD18:GR* transcripts to a level comparable to the *LBD18* transcript level of the wild-type plants (Fig. 8B). DEX treatment of *Pro*$_{35S}$*:LBD18:GR* in the *lbd18* mutant background resulted in a significant increase in the number of lateral roots (Fig. 8, C and D). A similar level of induction of lateral root formation was observed in the *lbd16 lbd18* double mutant background. No other significant phenotypes were detected with these transgenic mutants. These results show that LBD18 is responsible for its mutant phenotype and also that LBD18:GR is functional in lateral root formation. We found that while DEX treatment of *Pro*$_{35S}$*:LBD18:GR* in the *lbd18* mutant background can complement *lbd18* at almost a wild-type level, that of *Pro*$_{35S}$*:LBD18:GR* in *lbd16 lbd18* can induce lateral root formation at the same level as can be achieved by DEX treatment of *Pro*$_{35S}$*:LBD18:GR* in *lbd18* but cannot fully complement the *lbd16 lbd18* double mutants. These findings suggest that while LBD16 and LBD18 play roles in lateral root formation, they may also perform a distinctive role in a different pathway.

### *LBD18* Induces the Formation of Lateral Roots in *arf7 arf19* Mutants

The results of our earlier study demonstrated that the auxin up-regulated expression of *LBD16*, *LBD18*, and *LBD29* genes was repressed dramatically by DEX treatment and was inhibited completely by double mutations of *ARF7* and *ARF19*, thereby indicating that these *LBD* genes might be regulated by ARF7 and ARF19 in auxin signaling (Lee et al., 2009). It has also been previously reported that *LBD16* and *LBD29* overexpression induces lateral root formation in the absence of ARF7 and ARF19 and that dominant repression of *LBD16* inhibits lateral root formation (Okushima et al., 2007). To further demonstrate the positive role played by *LBD18* in lateral root formation, we constructed DEX-regulated *LBD18*-transgenic plants in the *arf7-1 arf19-1* mutant background (*Pro*$_{35S}$*:LBD18:GR/arf7 arf19*) by crossing these transgenic plants and mutants. The RT-PCR analysis of the *LBD18:GR* transcripts revealed fewer transcripts in *Pro*$_{35S}$*:LBD18:GR/arf7 arf19* compared with *Pro*$_{35S}$*:LBD18:GR* used for the construction of this transgenic mutant (Fig. 9A). As shown in Figure 9B, we noted a significant induction of lateral root numbers in *Pro*$_{35S}$*:LBD18:GR/arf7 arf19* after 12 d of DEX treatment, as compared with what was

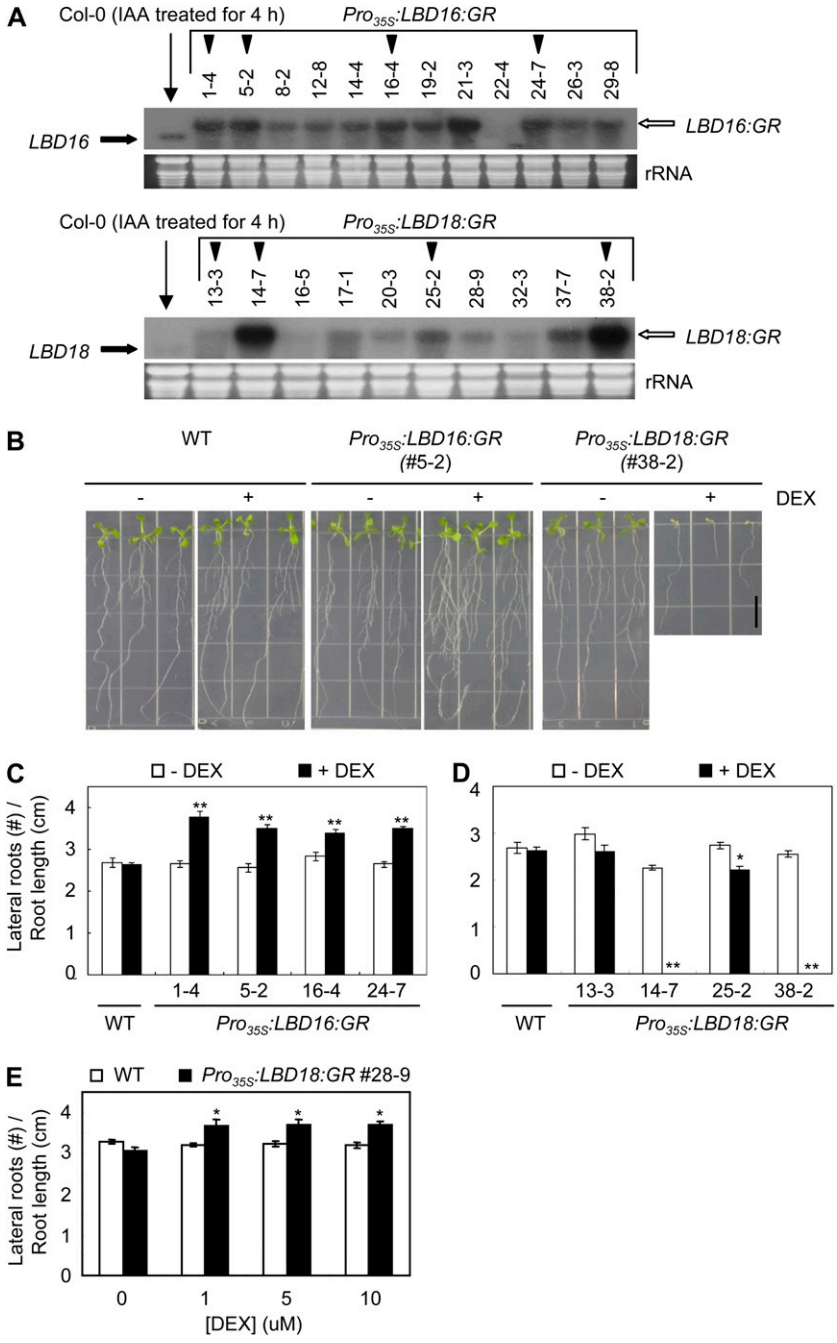


**Figure 6.** Analysis of lateral root numbers and primary root lengths in *Pro*$_{35S}$*:LBD16:GR* and *Pro*$_{35S}$*:LBD18:GR* transgenic plants. A, RNA gel-blot analysis of *LBD16*, *LBD18*, *LBD16:GR*, and *LBD18:GR* expression in wild-type, *Pro*$_{35S}$*:LBD16:GR*, and *Pro*$_{35S}$*:LBD18:GR* transgenic plants. Numbers above the top gels indicate the line numbers of homozygous transgenic Arabidopsis. Twenty micrograms of total RNA isolated from 10-d-old light-grown seedlings was subjected to RNA gel-blot analysis using *LBD16* or *LBD18* DNA probes. Transcripts of *LBD16* and *LBD18* are indicated by a thick black arrow, and the corresponding *GR* fusion transcripts are indicated by the white arrow. The black triangles indicate the Arabidopsis transgenic lines used for phenotypic analysis. Total RNA from wild-type plants was isolated from plants treated for 4 h with 20 $\mu$M IAA. B, Representative seedlings of *Pro*$_{35S}$*:LBD16:GR* and *Pro*$_{35S}$*:LBD18:GR* treated without or with DEX. Numbers in parentheses indicate the line numbers of Arabidopsis transgenic plants. Plants were grown vertically for 8 d in the absence (−) or presence (+) of 10 $\mu$M DEX. WT, Wild type. C, Lateral root numbers of various lines of *Pro*$_{35S}$*:LBD16:GR* transgenic plants without or with DEX. Plants were grown vertically for 8 d in the absence or presence of 10 $\mu$M DEX, and lateral root numbers per unit root length (cm) measured were plotted. Error bars indicate SE. $n > 20$. Asterisks denote statistical significance at $P < 0.01$. D, Lateral root numbers of various lines of *Pro*$_{35S}$*:LBD18:GR* transgenic plants without or with DEX. Plants were treated as described in the legend of Figure 7C. $n > 20$. Asterisks denote statistical significance at $P < 0.05$. Numbers below the columns in C and D indicate the line numbers of Arabidopsis transgenic plants. E, Lateral root numbers of line 28-9 of *Pro*$_{35S}$*:LBD18:GR* transgenic plants without or with DEX. Plants were grown vertically for 8 d with varying concentrations of DEX, and lateral root numbers per unit root length (cm) measured were plotted. $n > 21$. [See online article for color version of this figure.]

observed in the absence of DEX and in both the presence and absence of DEX in the *arf7 arf19* mutants. DEX treatment of wild-type plants did not affect lateral root number (data not shown). These results reveal that *LBD18* positively regulates lateral root formation downstream of *ARF7* and *ARF19*.

## DISCUSSION

Recent studies have demonstrated the functions of some *LBD* genes in lateral organ development in Arabidopsis and in crop plants, such as rice and maize (*Zea mays*). For many Arabidopsis *LBD* genes, loss-of-function mutation phenotypes were not apparent with the exception of *LBD6*, which performs a role in leaf development (Semiarti et al., 2001; Xu et al., 2003). However, several loss-of-function mutants of rice and maize *LBD* genes have been reported to evidence clear phenotypes (Inukai et al., 2005; Liu et al., 2005; Bortiri et al., 2006; Evans, 2007; Taramino et al., 2007). The ectopic expression of several *LBD* genes, as wild type or as proteins fused to a transcriptional repression domain, yielded morphological phenotypes, provid-

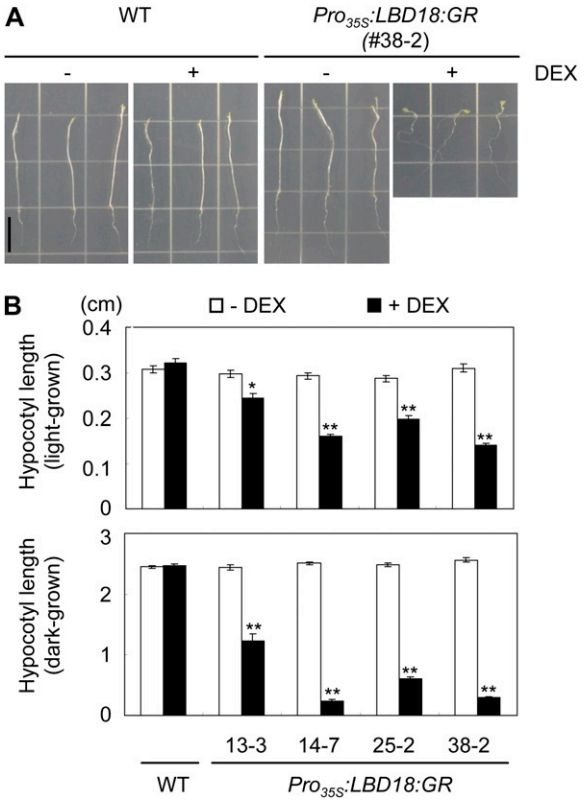


**Figure 7.** Hypocotyl lengths of $Pro_{35S}$:*LBD18*:*GR* transgenic plants. A, Representative plants of 7-d-old dark-grown $Pro_{35S}$:*LBD18*:*GR* plants treated without or with DEX. B, Hypocotyl lengths of 7-d-old light- or dark-grown $Pro_{35S}$:*LBD18*:*GR* plants treated without or with DEX. $n > 20$. WT, Wild type. Error bars indicate SE. Asterisks denote statistical significance at $P < 0.05$ (*) and $P < 0.01$ (**). [See online article for color version of this figure.]

ing clues to the biological functions of these *LBD* genes (Shuai et al., 2002; Chalfun-Junior et al., 2005; Borghi et al., 2007; Okushima et al., 2007). For example, the overexpression of *LBD16* or *LBD29* induced lateral root formation in the absence of ARF7 and ARF19, and the dominant repression of LBD16 activity inhibited lateral root formation; these findings suggest that these LBDs function downstream of ARF7- and ARF19-dependent auxin signaling in lateral root formation (Okushima et al., 2007). In this study, we demonstrated that *LBD16* and *LBD18* are involved in lateral root formation at the emergence step, based on the results of analysis of *lbd16* and *lbd18* single or double loss-of-function mutants. *LBD18* overexpression using a DEX-inducible system was shown to complement lateral root formation in *lbd18* as well as the *lbd16 lbd18* mutants, without inducing any other phenotypes. *LBD18* overexpression also induced lateral root formation in *arf7 arf19* mutants with blocked lateral root formation. Collectively, these results suggest that *LBD18* performs a function in lateral root formation, particularly during the initiation and emergence steps, in conjunction with *LBD16* downstream of *ARF7* and *ARF19*.

The *lbd16 lbd18* double mutants exhibited substantially reduced numbers of lateral roots compared with the *lbd16* and *lbd18* single mutants (Fig. 2), thereby suggesting that *LBD16* and *LBD18* might function in a combinatorial manner in lateral root formation. Because we failed to detect a protein-protein interaction between LBD16 and LBD18 in a yeast two-hybrid assay (data not shown), LBD16 and LBD18 might function redundantly in different pathways or might require auxiliary factors for their functional interaction. Some degree of lateral root formation could still be detected in the *lbd16 lbd18* double mutants, thereby indicating the existence of additional components for lateral root formation.

In the transgenic line expressing appropriate levels of the *LBD18*:*GR* transcripts in the wild-type background, a statistically significant increase in lateral root number was induced by treatment with various concentrations of DEX (Fig. 6E). In contrast, the transgenic lines expressing higher levels of the *LBD18*:*GR* transcripts exhibited significantly halted root growth, significantly decreased numbers of lateral roots, and reduced hypocotyl length (Figs. 6 and 7; Supplemental Figs. S2 and S3). These strong phenotypes may be related to the effects of ectopic tracheary element-like cells in nonvascular cells, as reported previously (Soyano et al., 2008). These results also indicate that appropriate *LBD18* expression levels might be necessary for the induction of lateral root formation in wild-type plants. In order to further demonstrate that increased *LBD18* expression can stimulate lateral root formation and that LBD18 is responsible for the mutant phenotype, we generated the transgenic mutants $Pro_{35S}$:*LBD18*:*GR* in the *lbd18* mutant background as well as in the *lbd16 lbd18* mutant background that express the *LBD18*:*GR* transcripts at the wild-type level or slightly higher. We noted that DEX treatment can induce lateral root formation in both *lbd18* and *lbd16 lbd18* mutant backgrounds (Fig. 8, C and D), thus clearly demonstrating that LBD18 plays a role in lateral root formation. GUS expression detected in the developing lateral roots of $Pro_{LBD18}$:*GUS* seedlings (Fig. 3) is also consistent with the role of *LBD18* in lateral root formation. In previous studies, it has been determined that in $Pro_{LBD16}$:*GUS* seedlings, GUS expression can be detected in the lateral root primordium (Okushima et al., 2007). We determined that while the GUS expression of $Pro_{LBD16}$:*GUS* seedlings is strong in the root stele and the developing and fully emerged lateral roots, that of $Pro_{LBD18}$:*GUS* is restricted to the primordia and the emerging lateral roots and is not detected in the lateral root stele. These GUS expression patterns suggest that *LBD16* and *LBD18* may have overlapping functions in the formation of lateral roots and that *LBD16* may play an additional role in the continued growth of lateral roots compared with *LBD18*.

Lateral roots are formed from mature root pericycle cells located adjacent to the proxylem poles of the parent root (Casimiro et al., 2003). The developmental

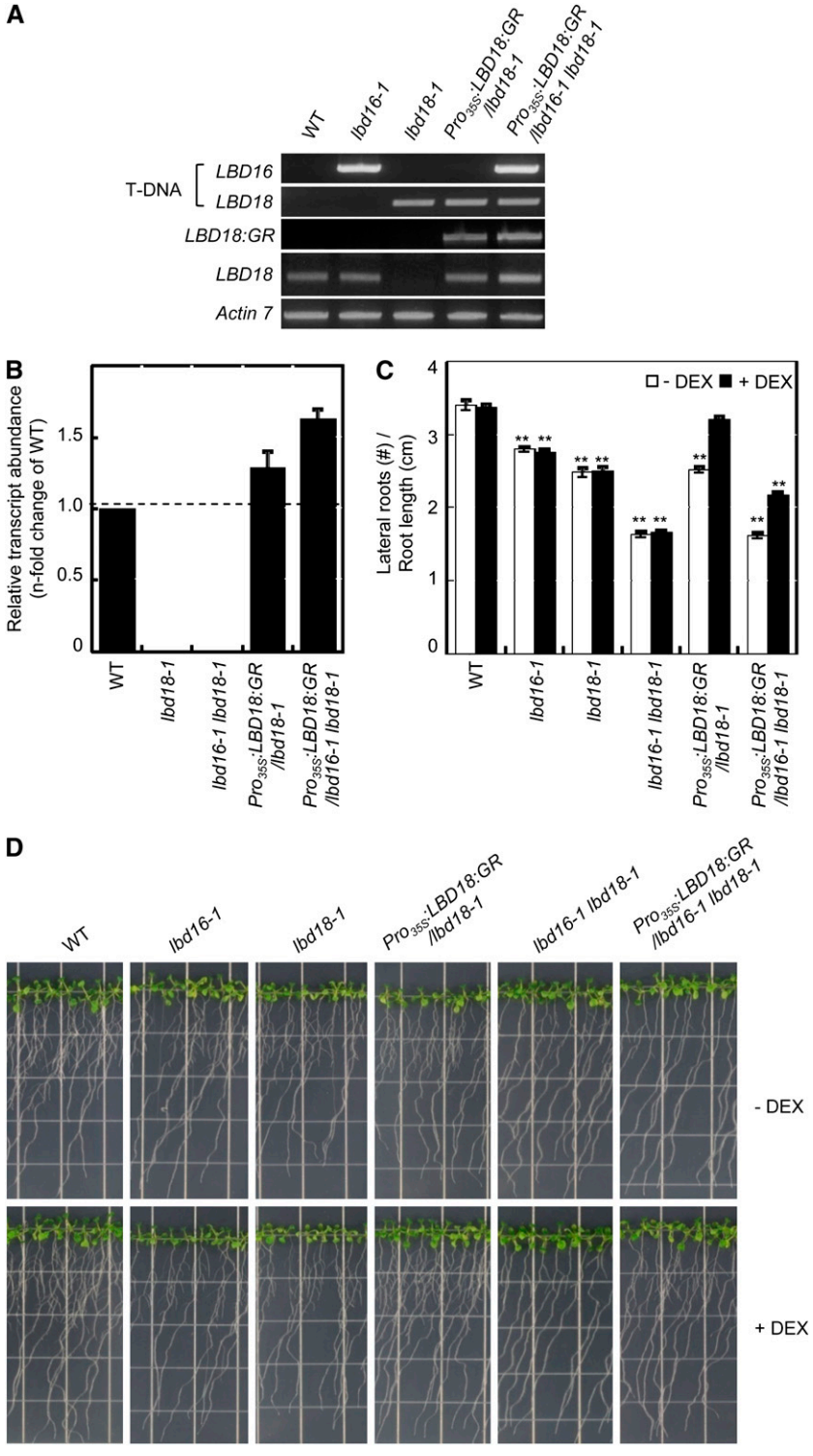


**Figure 8.** Complementation of *lbd18* or *lbd16 lbd18* by *LBD18:GR*. A, PCR analysis of $Pro_{35S}$:*LBD18:GR/lbd18-1* and $Pro_{35S}$:*LBD18:GR/lbd16-1 lbd18-1* transgenic mutants compared with *lbd18-1* and *lbd16-1 lbd18-1* mutants. Seven-day-old plants grown on Murashige and Skoog plates were harvested for genomic DNA followed by PCR analysis for T-DNA insertion, and total RNA was also isolated followed by RT-PCR analysis using the primers for the *LBD18:GR* fusion transcripts or the *LBD18* transcripts. *ACTIN7* mRNA was used as a loading control. WT, Wild type. B, Quantitative RT-PCR analysis of the *LBD18* transcripts in $Pro_{35S}$:*LBD18:GR/lbd18-1* and $Pro_{35S}$:*LBD18:GR/lbd16-1 lbd18-1* transgenic mutants compared with *lbd18-1* and *lbd16-1 lbd18-1* mutants. Relative abundance of the *LBD18* transcripts is shown compared with the wild type. C, Lateral roots of $Pro_{35S}$:*LBD18:GR/lbd18-1* and $Pro_{35S}$:*LBD18:GR/lbd16-1 lbd18-1* transgenic mutants compared with *lbd18-1* and *lbd16-1 lbd18-1* mutants without or with DEX. Plants were incubated and treated as described in Figure 6C, but for 12 d. Error bars indicate SE. $n > 24$. Asterisks denote statistical significance at $P < 0.01$. D, Lateral roots of transgenic mutants and wild-type plants. Photographs were taken 12 d after germination. [See online article for color version of this figure.]

events of lateral root formation include priming, initiation, primordium development, and the emergence of lateral roots (Fukaki and Tasaka, 2009). Recent studies with Arabidopsis have shown that auxin transport and signaling are necessary for lateral root initiation and primordium development. The auxin influx carrier, AUX1-dependent basipetal auxin transport, regulates the initiation of the lateral root (De Smet et al., 2007). The AUX1-like auxin influx carrier, LAX3 (for Like AUX1), promotes lateral root emergence (Swarup et al., 2008). Multiple *pin* mutations induced dramatic defects in root patterning, including the development of the lateral root primordium (Benková et al., 2003), thereby suggesting that auxin

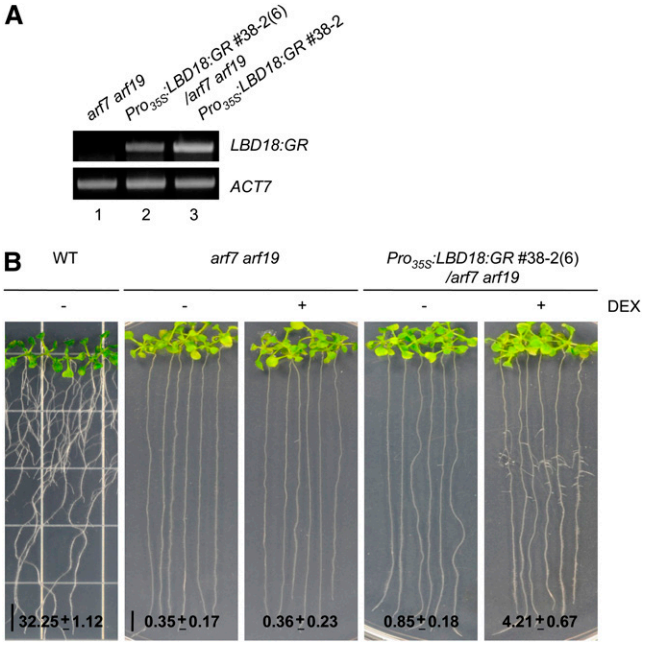


**Figure 9.** Induction of lateral roots in *arf7 arf19* mutants by activation of LBD18:GR with DEX treatment. A, RT-PCR analysis of $Pro_{35S}$:*LBD18*:*GR/arf7-1 arf19-1* transgenic mutants compared with *arf7 arf19* and $Pro_{35S}$:*LBD18*:*GR* for the *LBD18*:*GR* transcripts. Seven-day-old plants grown on Murashige and Skoog plates were harvested for total RNA followed by RT-PCR analysis using the primers for the *LBD18*:*GR* fusion transcripts. *ACTIN7* mRNA was used as a loading control. B, Lateral roots of $Pro_{35S}$:*LBD18*:*GR/arf7-1 arf19-1* transgenic mutants compared with *arf7 arf19* without or with DEX. Plants were incubated and treated as described in Figure 6C, but for 12 d. The numbers at bottom indicate average lateral root numbers ± SE. $n > 18$. WT, Wild type.

efflux regulated by PIN proteins is also required for lateral root formation. Auxin signaling mediated by the Aux/IAA and ARF families of transcriptional regulators has been determined to be required for lateral root formation. Various gain-of-function mutants of *Aux/IAA* genes, *slr-1*, *shy2/iaa3*, *msg2/iaa19*, *axr5/iaa1*, *iaa28*, and *crane/iaa18*, yielded dramatically reduced numbers of lateral roots (Tian and Reed, 1999; Rogg et al., 2001; Fukaki et al., 2002; Tatematsu et al., 2004; Yang et al., 2004; Uehara et al., 2008). Whereas mutations in ARF19 had little effect on their own and *ARF7* mutations resulted in impairments in hypocotyl phototropism, a variety of phenotypes that were not detected in these single mutants were observed in *arf7 arf19* double mutants, including reduction in lateral root formation (Harper et al., 2000; Okushima et al., 2005; Wilmoth et al., 2005), suggesting that *ARF7* and *ARF19* regulate lateral root formation in a redundant fashion. A novel regulator of lateral root primordium development, *PUCHI*, which encodes *AP2/EREBP*, has been identified and shown to play a role in lateral root morphogenesis by altering the pattern of cell division during the early stages of primordium development (Hirota et al., 2007). It has been suggested that *PUCHI* functions downstream of auxin signaling.

*LBD16* has been previously proposed to be involved in the initiation step of lateral root formation, based on the observation that the dominant repression of *LBD16* profoundly inhibited lateral root formation (Okushima et al., 2007). Our study involving loss-of-function mutant analysis demonstrated that, while the numbers of primordia of *lbd16* and *lbd18* single and double mutants were similar to those of the wild-type plants, the numbers of emerged lateral roots of the single mutants were reduced significantly compared with the wild type (Fig. 4A). In the *lbd16 lbd18* double mutants, additively reduced numbers of emerged lateral roots were noted as compared with the single mutants. Moreover, the numbers of primordia at stage I to stage VIII were not affected by *lbd16* and *lbd18* mutations (Fig. 4B). These findings reveal that *LBD16* and *LBD18* are likely to be involved in the initiation and emergence of lateral roots and to function additively in a different pathway. Recent study showed that GUS of $Pro_{LBD18}$:*GUS* transgenics is expressed in immature tracheary elements and that LBD18 functions in the differentiation of tracheary elements (Soyano et al., 2008). Therefore, it is possible that the phenotype of lateral root emergence in the *lbd16 lbd18* mutant might be related to the vascular differentiation in the lateral root primordium.

The results of microarray analysis demonstrated that the loss of *ARF7* and *ARF19* function completely suppressed the expression of *LBD16*, *LBD18*, and *LBD29* in response to auxin (Okushima et al., 2005). The ectopic expression of *LBD16* or *LBD29* in *arf7 arf19* mutants induced an increase in lateral root numbers (Okushima et al., 2007). We have also determined that ectopic *LBD18* expression in *arf7 arf19* mutants as the result of DEX treatment induced a significant increase in lateral root numbers (Fig. 9). Thus, we propose that *LBD16*, *LBD18*, and *LBD29* might act in a combinatorial fashion to regulate lateral root formation downstream of *ARF7* and *ARF19* during the auxin response. The results of our previous study demonstrated that the DEX-regulated expression of iaa1 with a domain II mutation resulted in a severe inhibition of lateral root formation and the suppression of *LBD16* and *LBD18* expression in response to auxin (Park et al., 2002; Lee et al., 2009). Reduced lateral root formation has also been noted in endogenous gain-of-function *iaa1/axr5* mutants (Yang et al., 2004). The *arf7* or *arf19* mutation resulted in a significant suppression of auxin-mediated *LBD16* expression (Lee et al., 2009). The expression of *LBD18* and *LBD29* in response to auxin in the *arf7* or *arf19* mutant was inhibited almost to basal levels (Lee et al., 2009). In the *arf7 arf19* double mutants, *LBD16*, *LBD18*, and *LBD29* expression was inhibited completely in response to auxin. In $Pro_{IAA1}$:*GUS* 7-d-old light-grown seedlings, we have detected strong GUS expression in various tissues, including the lateral roots (Lee et al., 2009). In $Pro_{ARF7}$:*GUS* and $Pro_{ARF19}$:*GUS* seedlings, GUS expression was also detected in various tissues, including the lateral roots, but the expression patterns of these two GUS fusion genes

are distinct. Partial overlap in the GUS of $Pro_{ARF7}$:*GUS* seedlings was detected in the root stele and in the developing lateral roots, whereas the GUS of $Pro_{ARF19}$:*GUS* seedlings was shown to be expressed in the entire region of the primary and lateral roots (Okushima et al., 2005). Collectively, these results indicate that *LBD16* and *LBD18* might be regulated downstream of the IAA1-ARF7/ARF19 transcriptional regulator system in auxin signaling to modulate lateral root formation at the initiation and emergence steps.

## MATERIALS AND METHODS

### Plant Growth and Tissue Treatment

Arabidopsis (*Arabidopsis thaliana*) seedlings were grown under a 16-h photoperiod and treated as described previously (Park et al., 2002).

### Plasmid Construction and Arabidopsis Transformation

The promoter region of *LBD16* or *LBD18*, which encompasses 1,416 bp from −1,436 to −20 bp or 2,034 bp from −2,054 to −20 bp relative to the AUG initiation codon, respectively, was isolated with PCR primers harboring *Hin*dIII (N terminus) and *Xma*I (C terminus) sites for *LBD16* and *Xba*I (N terminus) and *Xma*I (C terminus) sites for *LBD18* using the *Pfu* DNA polymerase (Stratagene) from the genomic DNA of Arabidopsis Col-0. These PCR products were inserted into pGEM-T Easy vector (Promega). The DNA fragments were cut with their corresponding restriction enzymes and subcloned into pBI101 (Clontech) in place of the cauliflower mosaic virus 35S promoter. The full-length *LBD16* and *LBD18* coding regions were synthesized via PCR using primers harboring *Xba*I (N terminus) and *Xho*I (C terminus), then ligated into *pBI-deltaGR* (Lloyd et al., 1994) as translational fusions with the GR hormone-binding domain to generate the constructs $Pro_{35S}$:*LBD16:GR* and $Pro_{35S}$:*LBD18:GR*, respectively. Transgenic Arabidopsis plants harboring these constructs ($Pro_{35S}$:*LBD16:GR* and $Pro_{35S}$:*LBD18:GR*) were then generated via *Agrobacterium tumefaciens*-mediated transformation (Bechtold et al., 1993). T3 homozygous transformants were generated and amplified (Park et al., 2002). All constructs were confirmed via DNA sequencing prior to plant transformation. The oligonucleotides utilized for PCR and the PCR conditions are provided in Supplemental Table S1.

### Isolation and Phenotypic Analysis of Arabidopsis *lbd16* and *lbd18* Single and *lbd16 lbd18* Double T-DNA Insertion Mutants

Arabidopsis *lbd16-1* (SALK_095791) and *lbd18-1* (SALK_038125) T-DNA insertion mutants from the Arabidopsis Biological Resource Center (ABRC) were verified by PCR with primers designed with the T-DNA primer design program, which is available from the Salk Institute Genomic Analysis Laboratory (http://signal.salk.edu/). The homozygous T-DNA insertion mutant lines were isolated with the primers shown in Supplemental Table S1. Double *lbd16 lbd18* mutants were generated by crossing of *lbd16-1* (female) with *lbd18-1* (male), and the resultant homozygous lines isolated were verified by PCR. Single-copy T-DNA in *lbd16* and *lbd18* was verified by backcrossing these mutants into wild-type plants and assessing the segregation of T-DNA by PCR. The null mutations of *lbd16*, *lbd18*, and *lbd16 lbd18* were further verified by RT-PCR analysis. Phenotypic analysis of these T-DNA insertion mutants was conducted for root length, hypocotyl length, number of lateral roots, gravitropic response, and morphological changes, as described previously (Park et al., 2002). For the analysis of the effects of 2,4-D on the lateral root number, we used 5-d-old seedlings grown vertically 4 d after transfer to the medium containing the indicated concentrations of 2,4-D (Dharmasiri et al., 2005).

### Generation of $Pro_{35S}$:*LBD18:GR* Transgenic Arabidopsis in *lbd18*, *lbd16 lbd18*, or *arf7 arf19* Mutant Backgrounds

Transgenic mutant $Pro_{35S}$:*LBD18:GR/lbd18* or $Pro_{35S}$:*LBD18:GR/lbd16 lbd18* was generated by crossing *lbd18-1* or *lbd16-1 lbd18-1* (female) with $Pro_{35S}$:*LBD18:GR* (male). Homozygous lines were isolated on the basis of genotyping and the PCR detection of genomic DNA for the *LBD18:GR* transgene. Expression levels of the *LBD18:GR* transcripts in Arabidopsis overexpressing $Pro_{35S}$:*LBD18:GR* in *lbd18-1* or *lbd16-1 lbd18-1* mutant were determined by RT-PCR analysis.

*arf7-1 arf19-1* mutants were acquired from the ABRC and confirmed by genotyping (http://signal.salk.edu) and lack of lateral root phenotype (Okushima et al., 2005). Arabidopsis overexpressing $Pro_{35S}$:*LBD18:GR* in *arf7-1 arf19-1* mutants was generated by crossing *arf7-1 arf19-1* (female) with $Pro_{35S}$:*LBD18:GR* (male). Homozygous lines were isolated according to genotype and lack of the lateral root phenotype for *arf7-1 arf19-1* and also by PCR detection of genomic DNA for the *LBD18:GR* transgene. Expression levels of the *LBD18:GR* transcripts in Arabidopsis overexpressing $Pro_{35S}$:*LBD18:GR* in *arf7-1 arf19-1* mutants were determined by RT-PCR analysis. The oligonucleotides and PCR conditions utilized are provided in Supplemental Table S1.

### RNA Isolation, RNA Gel-Blot Analysis, RT-PCR, and Real-Time RT-PCR

Following treatment, Arabidopsis plants were immediately frozen in liquid nitrogen and stored at −80°C. Total RNA was isolated from frozen Arabidopsis using TRI Reagent (Molecular Research Center). Total RNA was separated on a 1.2% agarose gel, transferred to nylon membranes, hybridized for 3 h with $^{32}$P-labeled DNA probes at 68°C using 10 mL of QuickHyb solution (Stratagene), and then washed. The blots were subsequently exposed to x-ray film. The DNA probes for RNA gel-blot analysis were RT-PCR amplified, subcloned into pGEM-T Easy vector (Promega), and then confirmed by DNA sequencing. For RT-PCR analysis, total RNA was isolated using an RNeasy Plant Mini kit (Qiagen) and subjected to RT-PCR analysis with an Access RT-PCR System (Promega) according to the manufacturer's instructions. Real-time RT-PCR was conducted with the QuantiTect SYBR Green RT-PCR kit (Qiagen) in a Rotor-Gene 2000 real-time thermal cycling system (Corbett Research). In order to determine the copy number of the transcripts in the treated sample, real-time PCR was performed on each sample with a known quantity of the in vitro transcribed RNA (Promega), yielding specific threshold values (Ct). A standard curve was generated to demonstrate the linear correlation between log(copy numbers of the RNA) and the Ct. The copy numbers of the transcripts of unknown samples were subsequently calculated from this standard curve. RT-PCR conditions, primer sequences, and DNA probes used in this study are provided in Supplemental Table S1.

### Nuclear Localization of EGFP:LBD18 Fusion Proteins in Arabidopsis Protoplasts

*LBD18* full-length DNA was PCR amplified using *Pfu* DNA polymerase (Stratagene) and inserted into the $Pro_{35S}$:*EGFP* vector (Lee et al., 2008) at the *Xho*I sites as a translational fusion, thereby yielding the $Pro_{35S}$:*EGFP:LBD18* DNA construct. PCR-amplified DNA sequences were used for subcloning after verification by DNA sequencing. These plasmids were purified using a Qiagen Plasmid Midi kit prior to protoplast transformation. The protoplasts from Arabidopsis mesophyll cells were prepared as described previously (Lee et al., 2008). Protoplasts isolated from the rosette leaves of 2- to 3-week-old Arabidopsis plants grown under a 16-h photoperiod were transfected with plasmid DNA by polyethylene glycol-mediated protoplast transformation and incubated for 18 h in the light at room temperature. The nuclear localization of the GFP fusion proteins was monitored by capturing GFP images with a TCS SP5 AOBS spectral confocal and multiphoton microscope system (Leica Microsystems). Confocal images of the GFP fusion proteins were acquired at the Korea Basic Science Institute. Argon (488 nm) and helium/neon (633 nm) lasers were utilized for GFP excitation and autofluorescence of chlorophyll excitation, respectively. Hoechst 33342 (Sigma) was utilized at 12 ng $mL^{-1}$ to stain the nuclei of the protoplasts. The protoplasts were incubated with Hoechst 33342 for 15 min at room temperature in darkness and rinsed three times in culture medium, and the excess buffer was drained and replaced with fresh culture medium.

### Statistical Analysis

Quantitative data on the phenotypes, such as measurements of root length, number of lateral roots, and hypocotyl length, were subjected to statistical

analysis for every pair-wise comparison using the software for Student's *t* test (Predictive Analytics Software for Windows version 17.0).

## Supplemental Data

The following materials are available in the online version of this article.

**Supplemental Figure S1.** Dose-response curves for root elongation of *lbd16*, *lbd18*, and *lbd16 lbd18* mutants on IAA.

**Supplemental Figure S2.** Lateral roots and primary root lengths of $Pro_{35S}$:*LBD16*:*GR* and $Pro_{35S}$:*LBD18*:*GR* transgenic plants.

**Supplemental Figure S3.** Root lengths of $Pro_{35S}$:*LBD18*:*GR* transgenic plants in the presence of varying concentrations of DEX.

**Supplemental Table S1.** Oligonucleotides used for PCR and PCR conditions.

## ACKNOWLEDGMENT

We thank the ABRC for the T-DNA insertion mutants utilized in this study.

Received June 25, 2009; accepted August 25, 2009; published August 28, 2009.

## LITERATURE CITED

**Bechtold N, Ellis J, Pelletier G** (1993) In planta Agrobacterium-mediated gene transfer by infiltration of adult Arabidopsis thaliana plants. C R Acad Sci (Paris) **316:** 1194–1199

**Benková E, Michniewicz M, Sauer M, Teichmann T, Seifertová D, Jürgens G, Friml J** (2003) Local, efflux-dependent auxin gradients as a common module for plant organ formation. Cell **115:** 591–602

**Borghi L, Bureau M, Simon R** (2007) *Arabidopsis* JAGGED LATERAL ORGANS is expressed in boundaries and coordinates KNOX and PIN activity. Plant Cell **19:** 1795–1808

**Bortiri E, Chuck G, Vollbrecht E, Rocheford T, Martienssen R, Hake S** (2006) *ramosa2* encodes a LATERAL ORGAN BOUNDARY domain protein that determines the fate of stem cells in branch meristems of maize. Plant Cell **18:** 574–585

**Casimiro I, Beeckman T, Graham N, Bhalerao R, Zhang H, Casero P, Sandberg G, Bennett MJ** (2003) Dissecting Arabidopsis lateral root development. Trends Plant Sci **8:** 165–171

**Chalfun-Junior A, Franken J, Mes JJ, Marsch-Martinez N, Pereira A, Angenent GC** (2005) ASYMMETRIC LEAVES2-LIKE1 gene, a member of the AS2/LOB family, controls proximal-distal patterning in Arabidopsis petals. Plant Mol Biol **57:** 559–575

**De Smet I, Tetsumura T, De Rybel B, Frey NF, Laplaze L, Casimiro I, Swarup R, Naudts M, Vanneste S, Audenaert D, et al** (2007) Auxin-dependent regulation of lateral root positioning in the basal meristem of Arabidopsis. Development **134:** 681–690

**Dharmasiri N, Dharmasiri S, Weijers D, Lechner E, Yamada M, Hobbie L, Ehrismann JS, Jurgens G, Estelle M** (2005) Plant development is regulated by a family of auxin receptor F box proteins. Dev Cell **9:** 109–119

**Evans MM** (2007) The indeterminate gametophyte1 gene of maize encodes a LOB domain protein required for embryo sac and leaf development. Plant Cell **19:** 46–62

**Fukaki H, Tameda S, Masuda H, Tasaka M** (2002) Lateral root formation is blocked by a gain-of-function mutation in the *SOLITARY-ROOT/IAA14* gene of Arabidopsis. Plant J **29:** 153–168

**Fukaki H, Tasaka M** (2009) Hormone interactions during lateral root formation. Plant Mol Biol **69:** 437–449

**Harper RM, Stowe-Evans EL, Luesse DR, Muto H, Tatematsu K, Watahiki MK, Yamamoto K, Liscum E** (2000) The *NPH4* locus encodes the auxin response factor ARF7, a conditional regulator of differential growth in aerial *Arabidopsis* tissue. Plant Cell **12:** 757–770

**Hirota A, Kato T, Fukaki H, Aida M, Tasaka M** (2007) The auxin-regulated AP2/EREBP gene *PUCHI* is required for morphogenesis in the early lateral root primordium of *Arabidopsis*. Plant Cell **19:** 2156–2168

**Husbands A, Bell EM, Shuai B, Smith HM, Springer PS** (2007) LATERAL ORGAN BOUNDARIES defines a new family of DNA-binding transcription factors and can interact with specific bHLH proteins. Nucleic Acids Res **35:** 6663–6671

**Inukai Y, Sakamoto T, Ueguchi-Tanaka M, Shibata Y, Gomi K, Umemura I, Hasegawa Y, Ashikari M, Kitano H, Matsuoka M** (2005) Crown rootless1, which is essential for crown root formation in rice, is a target of an AUXIN RESPONSE FACTOR in auxin signaling. Plant Cell **17:** 1387–1396

**Iwakawa H, Ueno Y, Semiarti E, Onouchi H, Kojima S, Tsukaya H, Hasebe M, Soma T, Ikezaki M, Machida C, et al** (2002) The ASYMMETRIC LEAVES2 gene of Arabidopsis thaliana, required for formation of a symmetric flat leaf lamina, encodes a member of a novel family of proteins characterized by cysteine repeats and a leucine zipper. Plant Cell Physiol **43:** 467–478

**Ku SJ, Park JY, Ha SB, Kim J** (2009) Overexpression of IAA1 with domain II mutation impairs cell elongation and cell division in inflorescences and leaves of Arabidopsis. J Plant Physiol **166:** 548–553

**Lee DJ, Kim S, Ha YM, Kim J** (2008) Phosphorylation of Arabidopsis response regulator 7 (ARR7) at the putative phospho-accepting site is required for ARR7 to act as a negative regulator of cytokinin signaling. Planta **227:** 577–587

**Lee DJ, Park JW, Lee HW, Kim J** (2009) Genome-wide analysis of the auxin-responsive transcriptome downstream of iaa1 and its expression analysis reveal the diversity and complexity of auxin-regulated gene expression. J Exp Bot **60:** 3935–3957

**Liu H, Wang S, Yu X, Yu J, He X, Zhang S, Shou H, Wu P** (2005) ARL1, a LOB-domain protein required for adventitious root formation in rice. Plant J **43:** 47–56

**Lloyd AM, Schena M, Walbot V, Davis RW** (1994) Epidermal cell fate determination in Arabidopsis: patterns defined by a steroid-inducible regulator. Science **266:** 436–439

**Malamy JE, Benfey PN** (1997) Organization and cell differentiation in lateral roots of Arabidopsis thaliana. Development **124:** 33–44

**Matsumura Y, Iwakawa H, Machida Y, Machida C** (2009) Characterization of genes in the ASYMMETRIC LEAVES2/LATERAL ORGAN BOUNDARIES (AS2/LOB) family in *Arabidopsis thaliana*, and functional and molecular comparisons between AS2 and other family members. Plant J **58:** 525–537

**Okushima Y, Fukaki H, Onoda M, Theologis A, Tasaka M** (2007) ARF7 and ARF19 regulate lateral root formation via direct activation of LBD/ASL genes in *Arabidopsis*. Plant Cell **19:** 118–130

**Okushima Y, Overvoorde PJ, Arima K, Alonso JM, Chan A, Chang C, Ecker JR, Hughes B, Lui A, Nguyen D, et al** (2005) Functional genomic analysis of the AUXIN RESPONSE FACTOR gene family members in *Arabidopsis thaliana*: unique and overlapping functions of ARF7 and ARF19. Plant Cell **17:** 444–463

**Park JY, Kim HJ, Kim J** (2002) Mutation in domain II of IAA1 confers diverse auxin-related phenotypes and represses auxin-activated expression of Aux/IAA genes in steroid regulator-inducible system. Plant J **32:** 669–683

**Rogg LE, Lasswell J, Bartel B** (2001) A gain-of-function mutation in *IAA28* suppresses lateral root development. Plant Cell **13:** 465–480

**Semiarti E, Ueno Y, Tsukaya H, Iwakawa H, Machida C, Machida Y** (2001) The ASYMMETRIC LEAVES2 gene of Arabidopsis thaliana regulates formation of a symmetric lamina, establishment of venation and repression of meristem-related homeobox genes in leaves. Development **128:** 1771–1783

**Shuai B, Reynaga-Pena CG, Springer PS** (2002) The lateral organ boundaries gene defines a novel, plant-specific gene family. Plant Physiol **129:** 747–761

**Soyano T, Thitamadee S, Machida Y, Chua NH** (2008) ASYMMETRIC LEAVES2-LIKE19/LATERAL ORGAN BOUNDARIES DOMAIN30 and ASL20/LBD18 regulate tracheary element differentiation in *Arabidopsis*. Plant Cell **20:** 3359–3373

**Swarup K, Benková E, Swarup R, Casimiro I, Péret B, Yang Y, Parry G, Nielsen E, De Smet I, Vanneste S, et al** (2008) The auxin influx carrier LAX3 promotes lateral root emergence. Nat Cell Biol **10:** 946–954

**Taramino G, Sauer M, Stauffer JL Jr, Multani D, Niu X, Sakai H, Hochholdinger F** (2007) The maize (Zea mays L.) RTCS gene encodes a LOB domain protein that is a key regulator of embryonic seminal and post-embryonic shoot-borne root initiation. Plant J **50:** 649–659

**Tatematsu K, Kumagai S, Muto H, Sato A, Watahiki MK, Harper RM, Liscum E, Yamamoto KT** (2004) *MASSUGU2* encodes *Aux/IAA19*, an auxin-regu-

lated protein that functions together with the transcriptional activator NPH4/ARF7 to regulate differential growth responses of hypocotyl and formation of lateral roots in *Arabidopsis thaliana*. Plant Cell **16:** 379–393

**Tian Q, Reed JW** (1999) Control of auxin-regulated root development by the Arabidopsis thaliana *SHY2/IAA3* gene. Development **126:** 711–721

**Uehara T, Okushima Y, Mimura T, Tasaka M, Fukaki H** (2008) Domain II mutations in CRANE/IAA18 suppress lateral root formation and affect shoot development in Arabidopsis thaliana. Plant Cell Physiol **49:** 1025–1038

**Wilmoth JC, Wang S, Tiwari SB, Joshi AD, Hagen G, Guilfoyle TJ, Alonso JM, Ecker JR, Reed JW** (2005) NPH4/ARF7 and ARF19 promote leaf expansion and auxin-induced lateral root formation. Plant J **43:** 118–130

**Xu L, Xu Y, Dong A, Sun Y, Pi L, Huang H** (2003) Novel as1 and as2 defects in leaf adaxial-abaxial polarity reveal the requirement for ASYMMETRIC LEAVES1 and 2 and ERECTA functions in specifying leaf adaxial identity. Development **130:** 4097–4107

**Yang X, Lee S, So JH, Dharmasiri S, Dharmasiri N, Ge L, Jensen C, Hangarter R, Hobbie L, Estelle M** (2004) The IAA1 protein is encoded by *AXR5* and is a substrate of $SCF^{TIR1}$. Plant J **40:** 772–782

**Yang Y, Yu X, Wu P** (2006) Comparison and evolution analysis of two rice subspecies LATERAL ORGAN BOUNDARIES domain gene family and their evolutionary characterization from Arabidopsis. Mol Phylogenet Evol **39:** 248–262